[AMERICAN JOURNAL OF SCIENCE, VOL. 266, MAY 1968, P. 342-360]

P–T–f_{O_2} RELATIONS FOR THE SYSTEM Fe–O–SiO_2

D. H. LINDSLEY,* D. H. SPEIDEL,** AND R. H. NAFZIGER***

ABSTRACT. Intensive-variable phase diagrams are receiving more frequent use by petrologists. Phase relations for the system Fe–O–SiO_2 expressed in P–T–f_{O_2} (intensive-variable) space provide a necessary building block for more complex but geologically important systems and also illustrate several important principles in the construction of such diagrams. The important phase relations for this system can be derived by application of Schreinemakers' rules to published experimental data obtained at 1 atm and a relatively few data obtained at high pressures.

Two invariant assemblages, each of five condensed phases, occur in the system: fayalite–silica–ferrosilite–iron–liquid at 17.5 kb, 1280°C, and $10^{-10.85}$ atm f_{O_2}; and fayalite–silica–ferrosilite–magnetite–liquid at 17 kb, 1205°C, and $10^{-7.25}$ atm f_{O_2}.

INTRODUCTION

This paper presents the phase relationships for the system Fe–O–SiO_2 in terms of the important intensive variables,[1] pressure, temperature, and oxygen fugacity (P, T, and f_{O_2}), for pressures below about 25 kb and oxygen fugacities below those at which hematite becomes stable. The phase relationships have been derived with the use of published experimental data, some new experimental data in the range 13 to 20 kb, and Schreinemakers' rules for the sequence of univariant curves around an invariant point. The diagrams presented in this paper were constructed to provide a basis for interpreting the phase relations in the geologically important system Fe–O–MgO–SiO_2 (Speidel and Nafziger, 1968). In addition, the diagrams provide excellent examples of several important concepts in the construction and interpretation of intensive-variable phase diagrams, and we have attempted to describe the relationships in sufficient detail that the arguments can be followed by a student who is just being introduced to Schreinemakers' rules and the concepts of degeneracy. It is our hope that this paper will prove useful in teaching the principles of phase diagrams.

The arguments presented below are based on several assumptions: (1) Except for wüstite (w), $Fe_{1-x}O$, which has a variable Fe:O ratio, and liquid (l), compositional variations in the phases are sufficiently small that they do not materially affect the phase diagrams. The remaining phases and their compositions are fayalite (o), Fe_2SiO_4; ferrosilite (p), $FeSiO_3$; magnetite (m), Fe_3O_4; iron (i), Fe; and silica polymorphs (s), SiO_2. The abbreviations for phases follow the usage of Speidel and

* Geophysical Laboratory, Carnegie Institution of Washington, Washington, D.C. 20008.

** Department of Geology, Queens College, Flushing, N.Y. 11367.

*** Department of Geochemistry and Mineralogy, Pennsylvania State University, University Park, Pa. 16802. Present address: U.S. Bureau of Mines, P.O. Box 70, Albany, Oregon 97321.

[1] Purists (personal commun., 1967) have correctly pointed out that *all* variables plotted as axes of phase diagrams are technically intensive variables: composition variables are intensive rather than extensive if they are expressed as fractions or percentages. Neverthless, it is still useful to distinguish between compositional variables and inherently intensive variables such as P, T, and f_{O_2}; only the latter type will be referred to as intensive variables in this paper.

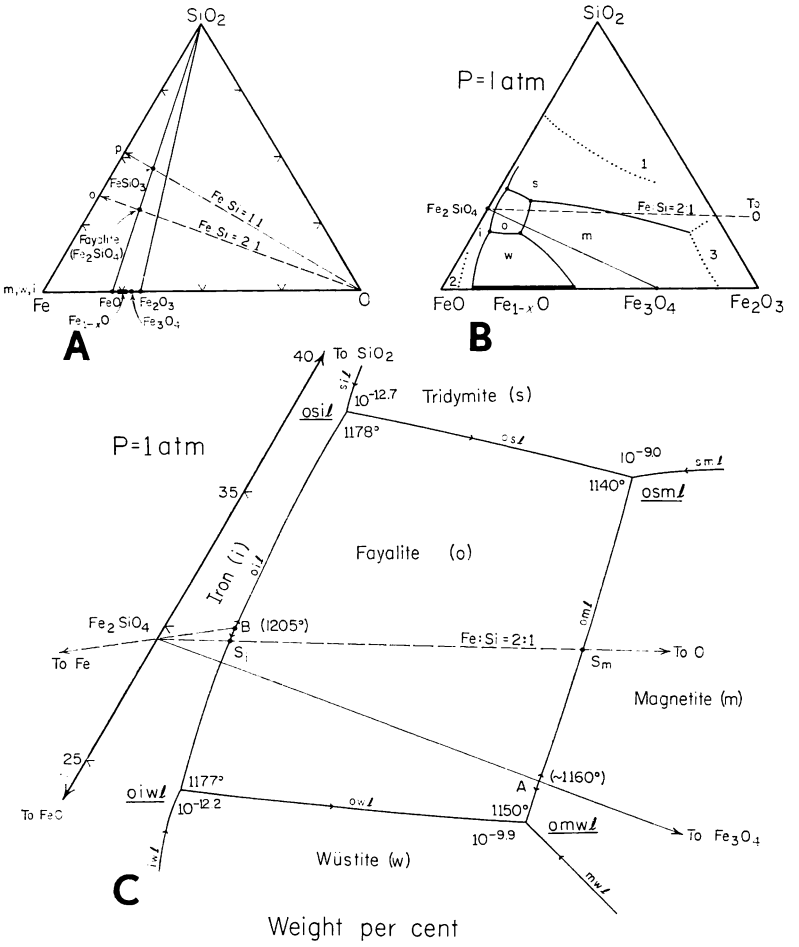

Fig. 1. Compositional relations in the system Fe–O–SiO_2. Abbreviations: m, magnetite; w, wüstite; i, metallic iron; o, fayalite; p, ferrosilite; l, liquid.

A. The system Fe–O–SiO_2 showing the subsystem FeO–Fe_2O_3–SiO_2 and the projection of the compositions Fe_2SiO_4 (fayalite) and $FeSiO_3$ (ferrosilite) from oxygen onto the Fe–SiO_2 join. Magnetite, wüstite, and iron all project onto the apex Fe.

B. The subsystem FeO–Fe_2O_3–SiO_2 as an equilateral triangle showing the liquidus relations at 1 atm total pressure. The dashed curve is the locus of all compositions with the ratio Fe:Si = 2:1. The dotted curves are (1) the silica–two-liquids boundary, (2) the iron–two-liquids boundary, and (3) magnetite–hematite–liquid and silica–hematite–liquid boundaries; these curves enclose the compositions (except for metallic iron) considered in this paper. After Muan (1955).

C. Enlargement of the area around the primary phase field of fayalite in B showing the temperatures (°C) and oxygen fugacities (atm) of the four isobarically invariant points involving fayalite. Data from Osborn and Muan (1960), except that the f_{O_2} for oiwl is from Darken and Gurry (1945). Arrows show directions of decreasing temperature along boundary curves; double arrows indicate temperature maxima at points A and B. Points S_i and S_m represent the liquids along curves oil and oml in which the Fe:Si ratio (2:1) is the same as that of fayalite.

Nafziger (1968). (2) The effects of polymorphism can be neglected. Both silica and ferrosilite have several polymorphic modifications in the pressure-temperature range considered here, but these polymorphic transitions should have a negligible effect on f_{O_2} relations. The effects of polymorphism on P–T diagrams are real (compare Lindsley, 1967, p. 228) but are ignored here. (3) The fields of liquid immiscibility can be ignored. In practice this is achieved by considering only those compositions on the silica-poor side of the two-liquids–cristobalite boundary curve (curve 1, fig. 1B) and on the oxygen-rich side of the two-liquids–iron curve (curve 2, fig. 1B). (4) There is no gas phase present. This assumption is rigorously correct only for the high-pressure experiments. In the experiments at 1 atm a gas phase consisting chiefly of components such as CO_2 and H_2 is added to the system as a device to regulate the intensive variable f_{O_2}.[2] But this added gas phase is no more a part of the experimental sample than is a furnace that regulates the intensive variable T or a piston that controls the intensive variable P. The gas phase is present *only* because extra components have been added as an experimental convenience; the partial pressures of the species in the ternary system Fe–O–SiO_2 total much less than 1 atm, and the gas phase of the ternary system can be neglected. Reactions and invariant points involving vapor as a phase are therefore omitted from this discussion.

GENERAL STATEMENT

The classic approach to phase relations in the system Fe–O–SiO_2 would be to view those relations in four-dimensional pressure-temperature-composition space, with axes P–T–X_1–X_2, where X_1 could be the join Fe–SiO_2 and X_2, the join Fe–O. The resulting diagram could be simplified by projecting all relations parallel to one composition axis—say X_2—into three-dimensional space. An additional projection parallel to the remaining composition axis would yield a two-dimensional diagram with the familiar intensive-variable axes P and T.

In recent years, however, there has been an increasing tendency for petrologists to plot compositional parameters as *intensive* variables; Korzhinskii (1959) has shown the theoretical basis for this practice and demonstrated its utility. There are cogent reasons for choosing oxygen fugacity (f_{O_2}) as an intensive variable for systems containing iron (or other transition elements): (1) There now exist several experimental techniques for controlling or measuring f_{O_2}. (2) During crystallization of

[2] Oxygen fugacity (f_{O_2}) is defined by the expression

$$\mu_{O_2} = \mu^\circ_{O_2} + RT \ln f_{O_2}$$

where μ_{O_2} is the chemical potential of oxygen, and $\mu^\circ_{O_2}$ is a constant representing the chemical potential of oxygen in some standard state. In an ideal gas phase the oxygen fugacity equals the partial pressure of oxygen. It should be noted, however, that a chemical potential (and therefore a fugacity) of oxgen can exist in the *absence* of a gas phase. Both μ_{O_2} and f_{O_2} are intensive variables reflecting the oxidizing or reducing (redox) tendency of the system. In this paper the variable f_{O_2} has been chosen because of its similarity to partial pressure, but all the diagrams would be qualitatively correct if the log f_{O_2} axes were replaced by μ_{O_2} axes.

some rocks, f_{O_2} has probably been externally imposed and thus was an important intensive variable controlling that crystallization. (3) Even in those rocks for which f_{O_2} was not externally imposed, knowledge of f_{O_2} relations derived from, say, the iron-titanium oxides may place important constraints on the interpretation of iron-bearing silicate assemblages in the same rock. The technique for converting oxygen from an extensive to an intensive compositional variable is simple: all compositions in a composition diagram are projected from oxygen (see, for example, Korzhinskii, 1959, p. 80-103). For the composition plane Fe–O–SiO_2, compositions may be projected from O onto the join Fe–SiO_2 (fig. 1A). This process of projection eliminates one composition axis, and in its place we may construct a new intensive-variable axis, that of f_{O_2}. We can now express the phase relations for the system Fe–O–SiO_2 in a four-dimensional diagram with axes P–T–f_{O_2}–X, where X is the line Fe–SiO_2. Projection of the phase relations parallel to X will eliminate the last extensive variable and will yield a three-dimensional intensive-variable diagram with the axes P–T–f_{O_2}. It is the purpose of this paper to investigate the phase relations of the system Fe–O–SiO_2 in the P–T–f_{O_2} space constructed in this manner.

At first it may seem of little consequence that we have projected the phase relations into P–T–f_{O_2} space rather than into P–T–X space. However, the geometric representation of phase assemblages is simplified in intensive-variable space: invariant assemblages appear as points, univariant assemblages as lines, and divariant assemblages as surfaces. Closely related to this is the fact that Schreinemakers' rules apply only to intensive-variable phase diagrams: the rules apply only in the P–T plane of P–T–X space, but they apply to *any* projection or section of P–T–f_{O_2} space. The ability to use this powerful tool in more than one plane provides a strong argument for the use of P–T–f_{O_2} space.

The system Fe–O–SiO_2 has three components, and thus a maximum of five phases can coexist in stable equilibrium. From the Gibbs phase rule—the variance equals 2 plus the number of components minus the number of phases—we see that for five-phase assemblages the variance is 0; that is, the values of all intensive parameters are fixed, and a given five-phase assemblage is stable only at a point in P–T–f_{O_2} space. Univariant, four-phase assemblages are stable along a line, and divariant, three-phase assemblages are stable upon a surface in that space. From each invariant point in a three-component system there radiate five univariant (four-phase) curves, each of which corresponds to a combination of four of the the five phases present at the invariant point. From each univariant curve there radiate four divariant (three-phase) surfaces, each of which corresponds to a combination of three of the four phases present along the univariant curve. Five-phase, four-phase, and three-phase assemblages will be termed, respectively, truly invariant, truly univariant, and truly divariant in this paper where necessary to

distinguish them from assemblages whose variance is reduced by arbitrarily fixing one of the intensive variables.

Most of the diagrams presented in this paper are projections of or sections through P–T–f_{O_2} space. Figures 3C and 4 are *projections*. The points, curves, and surfaces in P–T–f_{O_2} space project as points, curves, and surfaces; the variance is unchanged. Figures 2C and 5A to E, on the other hand, are isobaric, T–f_{O_2} *sections* through P–T–f_{O_2} space. Geometrically, a section corresponds to a plane normal to an axis at some fixed value of the parameter measured along that axis. We then view only that part of the phase diagram passing through that plane. By arbitrarily fixing the value of one intensive parameter in this way we reduce by 1 the variance of each element in the diagram.

A section will intersect each truly univariant curve at a point, which is invariant by restriction (in the isobaric example, a point becomes isobarically invariant); it will intersect each truly divariant surface in a line, which is univariant by restriction. (Only by "accident" will a section pass through a truly invariant point. Results of such "accidents" are shown in fig. 5.)

It will be of utmost importance in the following discussion to distinguish between projections and sections.

SCHREINEMAKERS' RULES

The laws governing the distribution of univariant curves about an invariant point were discovered by F. A. H. Schreinemakers and published in a number of articles, which appeared between 1915 and 1925.[3] These laws, commonly known as "Schreinemakers' rules", are the topologic expression of the fact that a given phase cannot partake in a stable reaction outside its own stability field. Zen (1966) has published an excellent summary of Schreinemakers' treatment; the reader should refer to Zen's paper and to Niggli (1954) for derivation of the rules.

The first rule, called the "fundamental axiom" by Zen (1966, p. 9), may be paraphrased:

"When two divariant assemblages, each of n phases, meet along a univariant curve of n + 1 phases, then on one side of the univariant curve the divariant assemblage I is stable relative to assemblage II, whereas on the other side of the curve assemblage II is stable relative to assemblage I".[4]

The second rule, the Morey-Schreinemakers' rule (Zen, 1966, p. 10-11), states that a divariant assemblage always occurs in a sector between two bounding univariant curves that make an angle no greater than 180°

[3] "In-, Mono-, and Di-Variant Equilibria," 29 papers in volumes 18 to 28 of the Proceedings of Koninklijke Akademie van Wetenschappen Te Amsterdam. Multilith copies are available at cost from College of Earth and Mineral Science, Experiment Station, The Pennsylvania State University, University Park, Pa. 16802.

[4] Zen's formulation of this rule refers to one assemblage being "relatively less metastable" than another and is correct in all cases. In the present paper we are concerned only with *stable* invariant points and the simpler phrase "stable relative to" is sufficient.

about the invariant point. (If the sector were greater than 180°, then in some part of the sector the divariant assemblage would be both stable and metastable.)

There are several elegant ways in which these rules may be used to determine the sequence of univariant curves about an invariant point—see, for example, Zen (1966, p. 12-14) and Niggli (1954, p. 403-412)—but we shall employ a simple technique. As each univariant curve corresponds to the absence of one of the phases of the invariant assemblage, we may label each curve with the symbol of the missing phase. Thus for the invariant assemblage ABCDE, the curve representing the univariant assemblage ABCD would be labeled (E). Curve (E) will be in the proper sequence when its metastable extension lies in the field where phase E can be stable, that is, on the same side as that where E appears for each of the other curves. When this condition holds for each of the curves, the entire sequence is correct.

Schreinemakers' rules give only the *sequence* of univariant curves about an invariant point. Additional data are needed to determine the *sense* of rotation of the univariant curves about the point. The rules apply to the sequence of univariant-by-restriction curves about invariant-by-restriction points as well as to truly univariant curves about truly invariant points.

T–f_{O_2} SECTION AT 1 ATMOSPHERE

A 1-atm section for the system Fe–O–SiO_2 intersects four truly univariant curves in P–T–f_{O_2} space, thus yielding four isobarically invariant points at each of which four phases coexist. Most of the available experimental data relate to this section, and it serves as a model for sections at higher pressures. All the necessary data are given by Bowen and Schairer (1932), Darken and Gurry (1945, 1946), Darken (1948), and Muan (1955), and are summarized by Osborn and Muan (1960) and in figure 1B-C. These data provide enough information on the f_{O_2}–T relations of the isobarically invariant points and univariant lines that it is possible to plot them directly on a T–f_{O_2} graph.

Figure 1C is a 1-atm liquidus diagram for part of the subsystem FeO–Fe_2O_3–SiO_2. The diagram is a temperature projection of a T-X-X isobaric section onto the X-X plane. Points osml, omwl, oiwl, and osil show, respectively, the compositions of the liquids in the isobarically invariant assemblages fayalite-silica-magnetite-liquid, fayalite-magnetite-wüstite-liquid, fayalite-iron-wüstite-liquid, and fayalite-silica-iron-liquid. The temperature and oxygen fugacity of each of these points are also presented in figure 1C. The four points can therefore be plotted on a T–f_{O_2} graph as in figure 2D. Because the data are for a fixed pressure of 1 atm, the resulting T–f_{O_2} diagram is a 1-atm isobaric section through P–T–f_{O_2} space. Note that each isobarically invariant point in figure 1C is surrounded by three isobarically univariant (three-phase) curves. The data of Muan (1955) permit us to plot these curves on the isobaric T–f_{O_2}

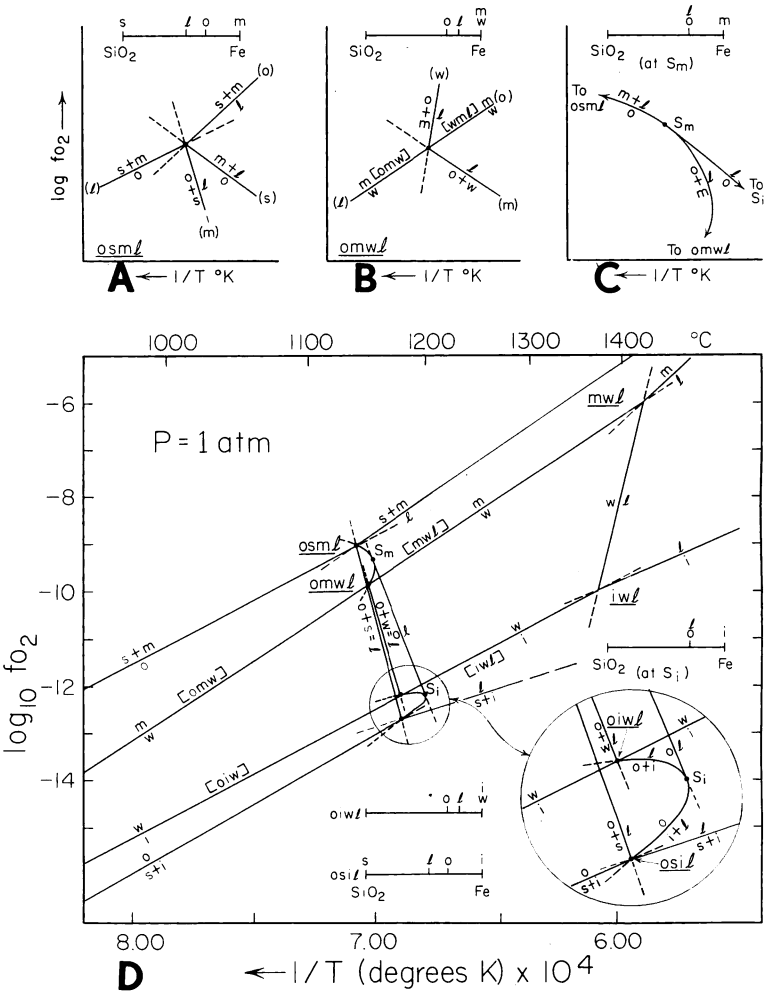

Fig. 2. T–f_{O_2} section through the system Fe–O–SiO_2 at 1 atm. Abbreviations as in figure 1. Composition lines show *relative* compositions of phases projected from O onto the Fe–SiO_2 join. Phase symbols in parentheses are those phases absent along each isobarically univariant curve. Short dashes are metastable portions of each isobarically univariant curve.

A. Sequence of isobarically univariant curves around point osml.

B. Sequence of isobarically univariant curves around point omwl. Because m and w have the same projected composition the diagram is degenerate: curve mw passes through omwl without inflection. The composition of the liquid lies between o and m or w, whereas that in figure 2A lies between o and s.

C. Relations along the curve oml near point S_m, where the projected compositions of o and l become identical. The curve o = l is the locus of all compositions in the primary field of fayalite with a Fe:Si ratio of 2:1.

D. One-atm isobaric T–f_{O_2} section for part of the system Fe–O–SiO_2. The inset shows details in the vicinity of points oiwl and osil. Points S_i and S_m are singular points and are discussed in the text. Possible ternary phase assemblages along the curves mw and iw are given in square brackets.

section (fig. 2D). Four of these curves—those for assemblages containing both fayalite and liquid—link the isobarically invariant points. Two of these four curves—oml and oil—pass through temperature maxima (points A and B in figs. 1C and 2D.) We have now plotted all information available from the 1-atm liquidus (T-X-X) diagram onto an intensive-variable diagram (T–f_{O_2} section, fig. 2D). Each four-phase isobarically invariant point in figure 2D should be surrounded by four three-phase curves. We obtained three curves for each point from the liquidus diagram; clearly the fourth curve for each point will be for a liquid-absent assemblage. The four missing curves are oxygen-buffer curves whose T–f_{O_2} relations are known (see the summary by Eugster and Wones, 1962, p. 90-92), and they can be plotted as curves o = s + m, m = w, i = w, and o = s + i in figure 2D.

We can now check to see whether the sequences of curves about the isobarically univariant points in figure 2D follow Schreinemakers' rules. In order to derive f_{O_2} as an intensive variable we projected compositions in the system Fe–O–SiO_2 from oxygen onto the Fe–SiO_2 join (fig. 1A). All phases with the same Fe:Si ratio project onto the same point, and *thus for the purpose of f_{O_2} diagrams* have the same composition, regardless of their actual oxygen content. Reactions between phases are also expressed as being independent of amounts of oxygen. Thus for the redox reaction

$$3Fe_2SiO_4 + O_2 = 2Fe_3O_4 + 3SiO_2$$

we will write equations only for the condensed phases

fayalite = magnetite + silica, or o = s + m.[5]

(The stoichiometric coefficients can be ignored for the purposes of this paper.) For any reaction, the bulk composition as projected onto the Fe-SiO_2 join must be maintained. Thus in the example given above the composition of fayalite must project between those of magnetite and silica.

Figure 2A is a T–f_{O_2} plot of relations close to the point osml; the curves are labeled with the appropriate reactions, and the compositions of the phases on the Fe–SiO_2 join are shown. Between each pair of isobarically univariant (three-phase) curves lies a divariant field corresponding to the two phases common to both curves. None of these divariant fields has an angular extent greater than 180°, so the Morey-Schreinemakers' rule is satisfied. Furthermore, the sequence of divariant fields and univariant curves satisfies the "fundamental axiom". By trying other sequences the reader can quickly convince himself that it is the only sequence consistent with the "fundamental axiom".

[5] The reader should bear in mind that in the absence of a gas phase or other reservoir of oxygen, the *extent* to which a redox reaction takes place will be limited, but the initial *direction* of the reaction will still depend on f_{O_2}. As oxygen is consumed or evolved, the f_{O_2} will change until an equilibrium value is reached; from then on the f_{O_2} is fixed by the assemblage until one or more condensed phases disappear. This, of course, is the principle of solid-solid oxygen buffers.

The construction of curves around the point omwl is closely similar to that around osml, with the important exception that the reaction m = w is independent of bulk composition. This independence arises from the coincidence of m and w in the composition projection from oxygen (figs. 1A, 2B). Because of this *degeneracy by coincidence,* only two phases are needed to define this isobarically univariant curve in the Fe–O–SiO_2 system. (See Niggli (1954, p. 387-390, 412-416) and Zen (1966, p. 30-40) for a further discussion of degeneracy.) Thus the reaction m = w is unaffected by the presence or absence of fayalite or liquid, and the m = w curve must pass through omwl without deflection (fig. 2B). We may think of this as two curves, each of which coincides with the other's metastable extension. At temperatures below that of omwl, liquid will not be stable, so the lower curve is labeled (l). Likewise, the portion of the m = w curve above oml is labeled (o), because fayalite would react with magnetite or wüstite to form liquid. The *assemblages* that are stable along the curves m = w in the Fe–O–SiO_2 system are shown in square brackets in figure 2A and D: assemblage omw is stable along the l-absent curve, and mwl along the o-absent curve. It is in degenerate phase diagrams of this sort that isobarically divariant fields (those of m and of w) attain the maximum angular extent—180°—permitted by the Morey-Schreinemakers' rule. The remaining curves about point omwl are (w) and (m); clearly, (w) must lie above and (m) below the m = w curve. Note that the composition of the liquid for omwl projects between fayalite and magnetite-wüstite (fig. 2B), so these curves must represent the reactions o + m = l and o+ w = l, and their metastable extensions will fall as in figure 2B.

The assemblage oml is common to osml and omwl, and thus the isobarically univariant curve oml must link those two isobarically invariant points (see the oml boundary curve in fig. 1C). However, the reaction leading from osml is o = m + l, whereas that from omwl is o + m =l. This change in reaction reflects the changing composition of the liquid from osml to omwl, as seen in projection from oxygen. There is one liquid—with an Fe:Si (atomic) ratio of 2:1—whose composition projects onto fayalite, and for this liquid the reaction simplifies to o = l. It is at the point S_m (figs. 1C, 2C) that the o = m + l and o + m = l curves join, and S_m is known as a singular point (Ricci, 1951, p. 61). Singularity occurs when a phase of variable composition incidentally attains the composition of another phase in the same reaction; on one side of the singular point the reaction is peritectic, such as o = m + l, whereas on the other side the reaction is eutectic, o + m = l. A third curve, o = l, tangent to both other curves, originates at the singular point (fig. 2C). The o = l curve is the locus of those liquids in the fayalite field of figure 1C with a 2:1 Fe:SiO_2 ratio. It might be noted that point S_m in figure 1C does not occur at the highest temperature along curve oml; the highest temperature occurs at point A where oml crosses the fayalite-magnetite join (fig. 1C).

The construction of curves around the points oiwl and osil is exactly analogous to that for omwl and osml and needs no further discussion. The results are summarized in figure 2D. Note that curve oil, like oml, has a singularity, S_i, the two points being joined by the curve o = l. That curve gives the maximum temperature stability of pure fayalite for any given value of f_{O_2}.

Curve o = l is closely similar to degenerate curves such as m = w and w = i in that the (projected) compositions of the two phases coincide, and only two phases are needed to define an isobarically univariant curve in a three-component system. Point S_i does not coincide with the highest temperature along curve oil; point S_i is the intersection of oil and the fayalite-oxygen join, whereas the maximum temperature (B in fig. 1C) is the intersection of oil and the extension of the fayalite-iron join. This fact was pointed out by D. C. Presnall (personal commun.).

P–T PROJECTION FOR THE SYSTEM Fe–O–SiO_2

The P–T diagrams discussed by Schreinemakers and Niggli are usually thought of as projections parallel to composition axes. As we are here considering relations in P–T–f_{O_2} space, we will be projecting parallel to the f_{O_2} axis onto the P–T plane. This is equivalent to projecting Fe–O–SiO_2 relations in P–T–X_1–X_2 space first from oxygen onto the Fe–SiO_2 join and then from iron onto the P–T plane as would be done in the standard projection from composition: the P–T projections obtained from the two methods will be identical. Because we are not dealing with f_{O_2} in this projection, compositions of phases must be expressed in a ternary diagram. For simplicity, reactions involving wüstite have been omitted.

There are two five-phase (invariant) assemblages of interest in the Fe–O–SiO_2 system, both of which involve the appearance of the pyroxene ferrosilite ($FeSiO_3$, here abbreviated p). Lindsley, MacGregor, and Davis (1964) located one of these points, opsil, at 17.5 kb and 1280°C. Lindsley (1967) discussed the P–T relations of the univariant curves around this point, treating the silicate phases as lying on the binary join FeO–SiO_2 and in equilibrium with metallic iron. Three of the curves emanating from this point have been determined experimentally. Nevertheless, it will be instructive to apply Schreinemakers' rules to the sequence of these univariant curves with the compositions treated as ternary rather than binary.

The compositions of the five phases are plotted in the subsystem Fe–Fe_2O_3–SiO_2 in figure 3A. Note that the phases i, s, o, and l lie at the apices of a quadrilateral and that the phase p lies within the quadrilateral and on a line between o and s. This *colinearity* of o, p, and s results in a degenerate phase diagram, in that a reaction involving only three phases—o, s, and p—defines a truly univariant curve in P–T projection. The curve o + s = p has been determined in equilibrium with metallic iron, but the iron does not enter the reaction and serves only to fix the

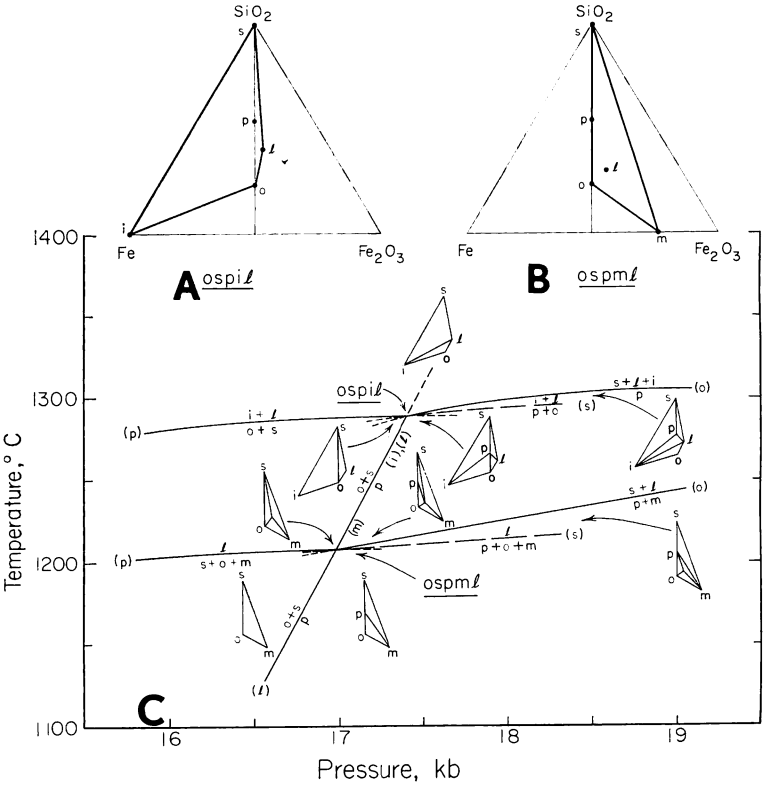

Fig. 3. P–T projection for part of the system Fe–O–SiO_2. Abbreviations as in figure 1.

A. Schematic representation of compositions of phases at point ospil in the join Fe–Fe_2O_3–SiO_2. Note that s, p, and o are colinear.

B. Schematic representation of compositions of phases at point ospml.

C. P–T projection of curves around points ospil and ospml. The assemblages stable between each pair of univariant curves are indicated by the composition diagrams. Curve o + s = p is degenerate in this projection and actually consists of three superimposed curves (see fig. 4). Phase symbols in parentheses indicate the phase of an invariant assemblage that is absent along each univariant curve. Curves opil and opml (shown by long dashes) have not been experimentally determined; their positions are closely constrained by the known positions of the other curves. Short dashes are metastable portions of each univariant curve.

f_{O_2} of the assemblage. At higher values of f_{O_2} the three-phase assemblage o + s = p remains stable in the absence of metallic iron, until at some still higher f_{O_2} the assemblage undergoes oxidation to form magnetite or liquid. The reaction o + s = p, which is rigorously univariant and therefore a line in P–T projection, is in P–T–f_{O_2} space a divariant surface that is rigorously parallel to the f_{O_2} axis. The surface is bounded at low values of f_{O_2} by the appearance of iron and at high values by the appearance of liquid or magnetite. Thus relative to the point ospil the reaction o + s = p in P–T projection can usefully be visualized as two

superimposed curves (l) and (i). This superposition of the stable portions of two curves reflects the degeneracy resulting from colinearity of three phases *within* the composition space. As we shall see for the point ospml. colinearity of phases *bounding* the composition space results in a different type of degeneracy.

Each univariant reaction around point ospil involves either the formation (or disappearance) of ferrosilite or the switching of tie lines, and these reactions are indicated graphically in figure 3C. The correct sequence of curves is given in this figure. Note that although the curve p + o = i + l has not been experimentally determined, its position near ospil is closely known, as its stable portion must lie below p = i + s + l and its metastable portion below i + l = s + o.

The compositions of the phases at the invariant point ospml are shown in figure 3B. The assemblage still contains the colinear phases s + p + o, but the osp line now forms one side of a composition triangle with m as the third apex and l as an interior phase. The colinearity is therefore bounding rather than internal as was the case for ospil. The resulting degeneracy finds a different expression in the P–T projection: The assemblage o + s can coexist with either m or l; also the phase p can coexist with either m or l. This fact can be expressed in the P–T projection if and only if the curve for the reaction o + s = p passes through the point ospml without inflection. This is equivalent to two curves, o + s = p (l absent) and o + s = p (m absent), each of which is coincident with the metastable portion of the other (fig. 3C) (the case is directly analogous to the m = w curve and the isobarically invariant point omwl (fig. 2B)). The other univariant reactions around ospml involve either the appearance of liquid or the switching of tie lines within the composition triangle o-s-m; the reactions and sequence of curves are shown in figure 3C.

Because the point ospml lies on the experimentally determined curve o + s = p, the P and T coordinates of ospml will be known if one of the other univariant curves is experimentally determined. Experimental data for the curves o + s + m = l and p + m = s + l are given in table 1. Point ospml lies at 1205° ± 15°C and 17 ± 0.5 kb. The completed P–T projection is shown in figure 3C.

T–f_{O_2} PROJECTION

If relations in P–T–f_{O_2} space are projected parallel to the pressure axis onto the T–f_{O_2} plane, a T–f_{O_2} projection is obtained (fig. 4). As in the P–T projection, univariant curves project as univariant curves. It should therefore be borne in mind that pressure, as well as temperature and f_{O_2} changes along each univariant curve. The most striking feature of figure 4 is the ruled surface representing the assemblage o + s + p. A divariant surface in P–T–f_{O_2} space, it separates the field of o + s at lower pressure from the field of p at higher pressure and is everywhere rigorously parallel to the f_{O_2} axis. As noted previously, the reaction o +

TABLE 1

Data on the reactions s + o + m = l and p + m = s + l

P ± 0.5 kb	T ± 10°C	Results
	Starting material: o+s+m	
13	1205	o+s+m
13	1215	o+s+l
16	1210	o+s+m
16	1220	s+l
16.5	1220	o+s+l
17	1210	o+s+m+p
	Starting material: s+l	
16	1195	o+s+m
	Starting material: p+m	
20	1235	p+m
20	1250	p+l+s

Abbreviations as in figure 1. Experiments were carried out with solid-media piston-and-cylinder pressure apparatus. Charge containers were platinum; alloying with platinum of some of the iron in the charge resulted in a small change in bulk composition; the change in composition was not enough to affect the results presented here.

s = p is univariant in terms of P and T but independent of f_{O_2} over a fairly wide range. The extent of the range can be seen from figure 4. At low values of f_{O_2} the ruled surface is terminated by the univariant curve opsi. At high values of f_{O_2} and at temperatures below that of the invariant point ospml the ruled surface is bounded by the univariant curve ospm. Between points ospml and ospil the ruled surface is terminated by the univariant curve ospl. Because these three bounding curves represent redox reactions, they are superimposed in P–T projection as the degenerate univariant curve o + s = p. Likewise, the reaction o + s = p cannot be expressed in f_{O_2}–T projection because the assemblage o + s is stable on one side of the ruled surface, say the front, and the phase p is stable on the other side.

It is noteworthy that although the four-phase *assemblage* remains unchanged for each univariant curve in P–T–f_{O_2} space, the *reaction* represented by that curve differs depending on how the curve is projected, that is, depending on which variables are chosen as independent. In P–T projection the curve spil is labeled p = s + l + i (fig. 3C); in T–f_{O_2} projection the same curve is labeled s + i = p + l (fig. 4), a redox reaction. In P–T projection the only reactions that can be represented are those involving changes in the *extensive* variables volume and entropy; the corresponding variables for T–f_{O_2} projection are entropy and oxygen content; and for P–f_{O_2} projection, volume and oxygen content. Therefore, although it is meaningful to speak only of an assemblage along a univariant curve in P–T–f_{O_2} space, it is valid to consider reactions across that curve in any *projection* of that space.

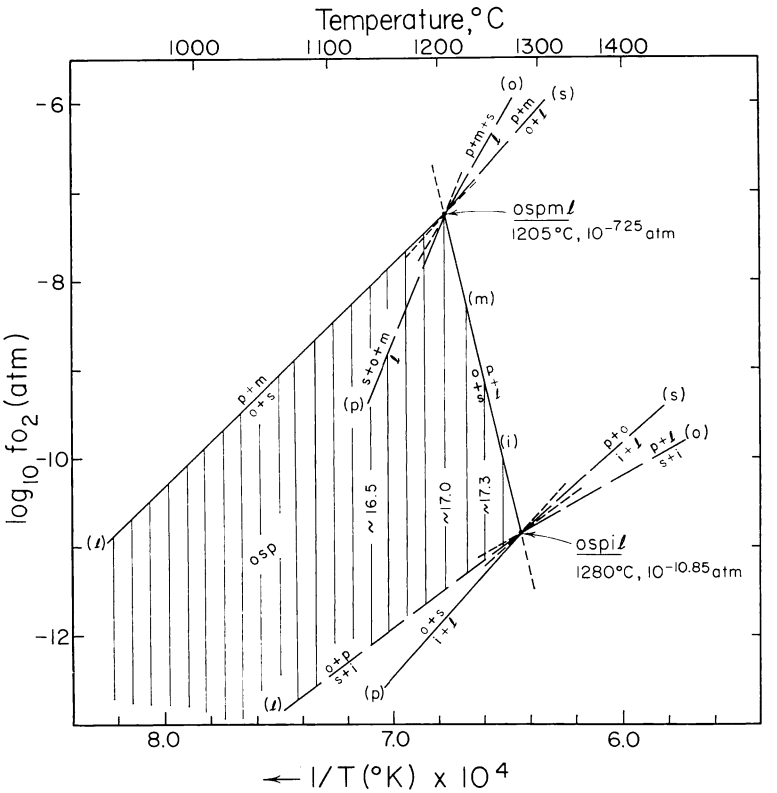

Fig. 4. Projection of part of the Fe–O–SiO_2 system parallel to the pressure axis onto the T–f_{O_2} plane. The f_{O_2} values for points ospml and ospil and the slopes for curves o + s = p + m and o + p = s + i are calculated from Eugster and Wones (1962, p. 90). Slopes for other curves are inferred. Many of the reactions shown along univariant curves are redox reactions, which cannot be shown in P–T projection (fig. 3). The ruled surface labeled osp is a divariant surface rigoriously parallel to the f_{O_2} axis. Each ruling represents the intersection of an isobaric plane with the surface osp in P–T–f_{O_2} space; several of these rulings are labeled with pressures corresponding to the isobaric sections in figure 5A to C.

Abbreviations as in figure 1. Phase symbols in parentheses represent the phase of a truly invariant assemblage that is absent along each univariant curve. Metastable portions of curves are dashed.

ISOBARIC (T–f_{O_2}) SECTIONS AT SEVERAL HIGH PRESSURES

We now have enough information to construct schematic T–f_{O_2} sections at high pressures to show how the relations in the 1-atm section (fig. 2D) are changed by the appearance of ferrosilite. There will be no qualitative changes at pressures below about 10 kb, the pressure at which ferrosilite becomes stable at room temperature. Sections at pressures from ~10 to less than 17 kb; at 17, 17.3, and 17.5 kb; and above 17.5 kb will be most useful. Curves for reactions involving wüstite are omitted for clarity. In all sections the curves o = m + l and o = i + l

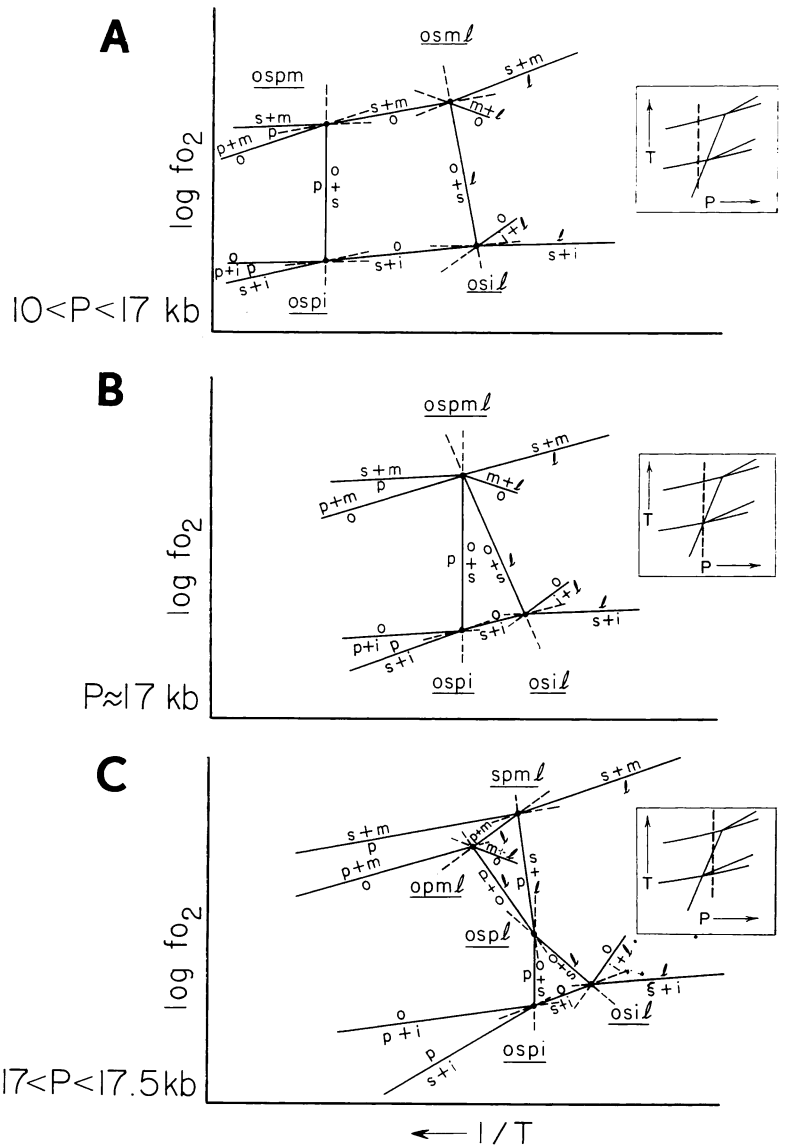
A
osmℓ
ospm
s+m
p+m
p
o
m+ℓ
p
o+s
ℓ
o+ℓ
s+i
p+i
ospi
osiℓ
log fo2
10<P<17 kb
T
P
B
ospmℓ
P≈17 kb
C
spmℓ
opmℓ
ospℓ
17<P<17.5kb
1/T

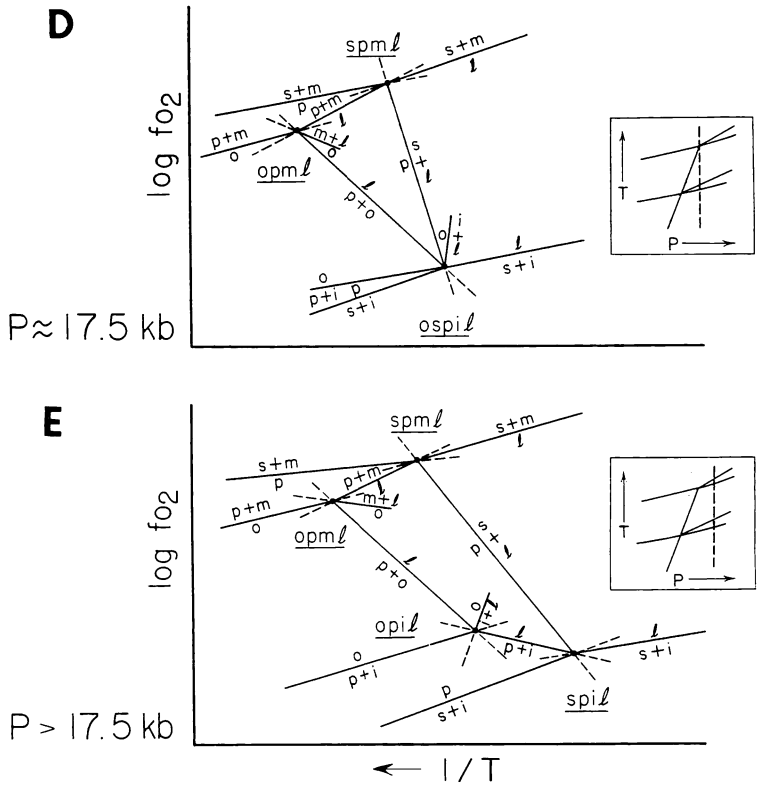

Fig. 5. Schematic isobaric sections through P–T–f_{O_2} space for the system Fe–O–SiO_2 at several high pressures. Insets show where each section is taken relative to the P–T projection (fig. 3C). Abbreviations as in figure 1. Metastable portions of curves are dashed. Equilibria involving wüstite are omitted, as are the singular points S_i and S_m (which would appear on the curves o = i + l and o = m + l) and the curve o = l, which connects S_i and S_m.

A. Section at approximately 16.5 kb to illustrate relations in the range ∽10 to less than 17 kb. Points osml and osil are present at 1 atm. Points ospm and ospi reflect the stability of ferrosilite at high pressures. Curve o + s = p is rigorously parallel to the f_{O_2} axis and is, for example, the vertical ruling labeled 16.5 kb in figure 4. Points ospm and ospi reflect the intersection of curve o + s = p (fig. 3C) at two different values of f_{O_2}.

B. Section at approximately 17 kb, the pressure of the invariant point ospml. The existence of six (isobarically) univariant curves around a (truly) invariant point is discussed in the text. The sequence of these six curves cannot be deduced from Schreinemakers' rules.

C. Section at approximately 17.3 kb to illustrate relations in the range >17 to <17.5 kb.

D. Section at approximately 17.5 kb, the pressure of the univariant point ospil. The sequence of the six (isobarically) univariant curves around ospil cannot be deduced from Schreinemakers' rules.

E. Section at approximately 18 kb to show relations in the pressure range above 17.5 kb.

will pass through singular points, yielding the same relations as illustrated in figure 2C-D; these, too, are omitted for clarity.

Figure 5A illustrates schematically the isobaric T–f_{O_2} relations at any pressure from 10 to nearly 17 kb. The isobaric section cuts four truly univariant curves in isobarically invariant points. Two of the curves—osil and osml—are also cut by the 1-atm section, and the sequences of curves around the resulting isobarically invariant points are identical with those in figure 2C. Two new isobarically invariant points —ospm and ospi—result from intersections with the univariant curves ospm and ospi (that is, the degenerate curves o + s = p when viewed in P–T projection). The curve o + s = p connecting ospm and ospi in figure 5A is rigorously parallel to the f_{O_2} axis and is thus independent of f_{O_2}; it is one of the vertical rulings—for example that labeled 16.5 kb—on the ruled surface in figure 4. Analysis of the sequence of curves around each invariant point is routine and need not be detailed here.

As pressure is increased, points ospm and osml move closer together, until at approximately 17 kb they merge into the truly invariant point ospml (fig. 5B). This is the lowest pressure at which ferrosilite is stable in the presence of liquid. The curve o = s + m disappears, but all other curves remain, with the apparently anomalous result that six univariant curves emanate from a single five-phase invariant point. That this result is correct can be seen from the following analysis: A five-phase invariant point has five truly univariant curves emanating from it, but because the slope dT/dP of each of these curves is generally not infinite, an isobaric *section* passed through the invariant point will intersect *none* of these truly univariant curves. The section will, however, intersect some divariant surfaces to yield isobarically univariant curves. Each pair of truly univariant (four-phase) curves is joined by a divariant surface representing the three-phase assemblage common to each. For example, the curves p + m = s + l and p + o + m = l in figure 3C are joined by the divariant surface for the assemblage pml. Around point ospml there are ten such divariant surfaces: pml, sml, spl, spm, oml, opl, opm, osl, osm, and osp. However, if both the bounding univariant curves of a divariant surface lie at pressures either above or below the pressure of ospml, the stable portion of the divariant surface will not be cut by the isobaric section through the invariant point. There are four such surfaces: osm lies entirely at pressures below, and spl, opl, and pml at pressures above, ospml. The remaining six surfaces *are* intersected, yielding the six isobarically univariant curves in figure 5B. Thus we see that the "accident" of passing an isobaric section through a truly invariant point yields a T–f_{O_2} section in which six isobarically univariant curves emanate from the five-phase invariant point. Note that the surface osm was intersected in the section below 17 kb (fig. 5A), yielding the isobarically univariant curve o = s + m. The sequence of all isobarically univariant curves about a truly invariant point as in figure 5B cannot be directly determined by applying Schreinemakers' rules.

The correct sequence can be obtained, however, allowing figures 5A and C to approach 17 kb and observing the distribution of isobarically univariant curves associated with the five isobarically invariant points ospm, osml, opml, spml, and ospl.

At 17 kb, as at all other pressures, the curve o + s = p is parallel to the f_{O_2} axis.

An isobaric section at a pressure between 17 and 17.5 kb cuts the three remaining divariant surfaces associated with ospml: pml, spl, and opl. The section also cuts the truly univariant curves p + o + m = l, p + m = s + l, and o+ s = p + l, yielding three new isobarically invariant points: opml, psml, and ospl (fig. 5C).

An isobaric section at approximately 17.5 kb, the pressure of point ospil, yields another diagram in which a truly invariant point is surrounded by six isobarically univariant curves (fig. 5D). At and above 17.5 kb the assemblage s + o is not stable, so the vertical curve s + o = p has disappeared.

The isobaric section for pressures greater than 17.5 kb (fig. 5E) needs no special discussion.

CONCLUSIONS

The P–T–f_{O_2} relations of the system Fe–O–SiO_2 provide excellent illustrations of several principles of intensive-variable phase diagrams. Among these are application of Schreinemakers' rules, derivation of singular points, degenerate equilibria due both to coincidence and to colinearity, the different reactions represented by different projections of the same univariant curve, and the nature of univariant-by-restriction curves in a section through a truly invariant point. The illustrations should prove useful in teaching these concepts.

The geologic implications of the results of this paper are discussed by Speidel and Nafziger (1968) in the following paper.

ACKNOWLEDGMENTS

We are indebted to a large number of our colleagues for stimulating discussions of the material in this paper. By their penetrating but constructive criticism of the manuscript, G. W. Fisher, S. A. Morse, and E. H. Roseboom greatly improved its content and clarity. Our deep thanks go to them all.

REFERENCES

Bowen, N. L., and Schairer, J. F., 1932, The system FeO–SiO_2: Am. Jour. Sci., 5th ser., v. 24, p. 177-213.

Darken, L. S., 1948, Melting points of iron oxides on silica: Phase equilibria in the system Fe–Si–O as a function of gas composition and temperature: Am. Chem. Soc. Jour., v. 70, p. 2046-2053.

Darken, L. S., and Gurry, R. W., 1945, The system iron-oxygen. I. The wüstite field and related equilibria: Am. Chem Soc. Jour., v. 67, p. 1398-1412.

———— 1946, The system iron-oxygen: II. Equilibria and thermodynamics of liquid oxides and other phases: Am. Chem. Soc. Jour., v. 68, p. 798-816.

Eugster, H. P., and Wones, D. R., 1962, Stability relations of the ferruginous biotite, annite: Jour. Petrology, v. 3, p. 82-125.

Korzhinskii, D. S., 1959, Physicochemical basis of the analysis of the paragenesis of minerals: New York, Consultants Bureau, 142 p.

Lindsley, D. H., 1967, Pressure-temperature relations in the system FeO-SiO_2: Carnegie Inst. Washington Year Book 65, p. 226-230.

Lindsley, D. H. MacGregor, I. D., and Davis, B. T. C., 1964, Synthesis and stability of ferrosilite: Carnegie Inst. Washington Year Book 63, p. 174-176.

Muan Arnulf, 1955, Phase equilibria in the system FeO–Fe_2O_3–SiO_2: Am. Inst. Mining Metall. Engineers Trans., v. 203, p. 965-976.

Niggli, Paul, 1954, Rocks and mineral deposits: San Francisco, California, W. H. Freeman and Company, 559 p.

Osborn, E. F., and Muan, Arnulf, 1960, Phase equilibrium diagrams of oxide systems, Plate 6, The system FeO–Fe_2O_3–SiO_2: Columbus, Ohio, Am. Ceramic Soc. and the Edward Orton, Jr., Ceramic Found.

Ricci, J. E., 1961, The phase rule and heterogeneous equilibrium: New York, Van Nostrand and Company, 505 p.

Speidel, D. H., and Nafziger, R. H., 1968, P–T–f_{O_2} relations in the system Fe–O–MgO–SiO_2: Am. Jour. Sci., v. 266, p. 361-379.

Zen, E-an, 1966, Construction of pressure-temperature diagrams for multicomponent systems after the method of Schreinemakers: A geometric approach: U.S. Geol. Survey Bull. 1225, 56 p.